

On the Experimental Estimation of Surface Enhanced Raman Scattering (SERS) Cross Sections by Vibrational Pumping

R. C. Maher* and L. F. Cohen

*The Blackett Laboratory, Imperial College London
Prince Consort Road, London SW7 2BW, United Kingdom*

E. C. Le Ru and P. G. Etchegoin†

*The MacDiarmid Institute for Advanced Materials and Nanotechnology
School of Chemical and Physical Sciences, Victoria University of Wellington, PO Box 600 Wellington, New Zealand
(Dated: December 2, 2024)*

We present an in-depth analysis of the experimental estimation of cross sections in Surface Enhanced Raman Scattering (SERS) by vibrational pumping. The paper highlights the advantages and disadvantages of the technique, pinpoints the main aspects and limitations, and provides the underlying physical concepts to interpret the experimental results. Examples for several commonly used SERS probes are given, and a discussion on future possible developments is also presented.

PACS numbers: 78.67.-n, 78.20.Bh, 78.67.Bf, 73.20.Mf

I. INTRODUCTION

In the last decade Surface Enhanced Raman Scattering (SERS)[1] has made rapid progress towards applications. With a sensitivity rivalling fluorescence in some cases, and a much higher structural specificity, SERS is a highly attractive technique, being developed simultaneously with the field of plasmonics. Progress towards different uses of SERS in practical applications has been steady. New substrates including: arrays of inverted pyramids[2], silver pillar and torroid arrays[3], adaptive silver films[4], and metallic nano-shells[5], have been demonstrated. In addition, many molecules relevant to a myriad of applications such as glucose[6], proteins[7], DNA[8], a wide range of medicinal drugs[9, 10, 11], and substances for forensic science[12], have been characterized. On the other hand, the understanding of some fundamental aspects of the phenomenon has been slow, and in some cases controversial. Although a full understanding is sometimes not essential for the development of applications, there can be no denying in the fact that a full comprehension is desirable.

Optical pumping of vibrational modes was first suggested in 1996 based on the observed dependence of the anti-Stokes/Stokes (aS/S) ratio with incident laser power[13], and it was suggested that this could be a possible tool to estimate SERS cross sections. However, the interpretation of the experimental results have been the subject of considerable debate in the literature, with many authors simply denying its existence and attributing the experimental observations to either laser-heating, resonance effects, or combinations thereof[14, 15, 16, 17].

Over a series of previous papers we have suggested the investigation of the aS/S-ratio as a function of temperature (T) as an alternative method for the observation of pumping[18, 19, 20]. In a recent paper, we provided what we believe is a definitive proof for vibrational pumping under SERS conditions using this technique[20]. Accordingly, we provide here an in-depth discussion on the state of the state-of-the-art of cross section estimation in SERS via vibrational pumping, and extend the method to different analytes, and laser excitations. We also address several outstanding issues which were not considered previously[20]. Before we go into the details, we briefly review the necessary concepts for understanding aS/S-ratios and vibrational pumping in SERS. The method we are going to discuss has not been used much by other authors and, therefore, we review not only the historical background that led to this method, but also its peculiarities and limitations to set the ground for future developments. The discussion has some natural overlap with our previous papers[18, 19, 20] but it is presented here for the sake of completeness, the convenience of the reader, and future reference for forthcoming work in progress. This will inevitably result in a somewhat lengthy introductory section where the principles of the method are laid down. The next sections are fully devoted to this and are followed by a section at the end with a practical experimental demonstration of SERS cross section determination for several standard probes.

II. A BRIEF DESCRIPTION OF SERS PUMPING

A. The Anti-Stokes/Stokes ratio

Let us consider the different contributions to the population of a single vibrational level at temperature T dur-

*Electronic address: Robert.Maher@imperial.ac.uk

†Electronic address: Pablo.Etchegoin@vuw.ac.nz

ing a SERS measurement; we can identify two main contributions: (i) the laser itself which pumps vibrations through Raman processes with a rate proportional to its intensity (I_L) and to the Raman-Stokes cross section (σ_S), and (ii) thermal excitation and relaxation. Vibrations remain in the level with a finite lifetime τ , which encompasses all possible relaxation mechanisms –such as intramolecular vibrational relaxation IVR (anharmonic processes) or external relaxation mechanisms. There are other possible secondary mechanisms, such as relaxation through an anti-Stokes Raman processes, or excitation to higher vibrational levels. It is possible to write rate equations for the detailed dynamics of vibration populations in such a system [16]. In the regime of weak pumping (which is the only case considered here), where the vibrational population remains small, $n \ll 1$, it is sufficient to consider only the two main mechanisms, and the rate equation for n can then be written as:

$$\frac{dn}{dt} = \frac{\sigma_S I_L}{\hbar\omega_L} + \frac{\exp(-\hbar\omega_\nu/k_B T)}{\tau} - \frac{n}{\tau}, \quad (1)$$

where σ_S is the Raman-Stokes cross section, I_L the intensity (power per surface area) of the laser, $\hbar\omega_L$ the energy of an exciting photon ($n_L = I_L/\hbar\omega_L$ is the number of incident photon per unit time and surface area), and $\hbar\omega_\nu$ the energy of the vibration. The first term on the right is the number of vibrations per unit time being pumped into the level by the action of the laser, while the second and third terms are the contributions of thermal excitation and population relaxation, respectively. In the steady state $dn/dt = 0$. Generally, σ_S is very small, so when I_L is small the pumping contribution is negligible and the vibrational population is dominated by thermal effects; i.e. $n = \exp(-\hbar\omega_\nu/k_B T)$ is given by a Boltzmann factor. When I_L is increased (so that there is a significant pumping contribution to the population of the level) n becomes:

$$n = \frac{\tau\sigma_S I_L}{\hbar\omega_L} + e^{-\hbar\omega_\nu/k_B T}, \quad (2)$$

where the pumping term is clearly distinguished from the thermal contribution.

In addition, for an ensemble of N molecules, the Stokes-Raman signal is given by $I_S = N\sigma_S I_L$ while the anti-Stokes signal is given by $I_{aS} = nN\sigma_{aS} I_L$, leading to:

$$I_{aS} = \left(\frac{\tau\sigma_S I_L}{\hbar\omega_L} + e^{-\hbar\omega_\nu/k_B T} \right) N\sigma_{aS} I_L. \quad (3)$$

Moreover, taking the ratio of the anti-Stokes to the Stokes intensities (ρ), we have:

$$\rho = \frac{I_{aS}}{I_S} = \frac{\sigma_{aS}}{\sigma_S} n = An, \quad (4)$$

where A is the *asymmetry factor* (extensively discussed in Refs. [18, 19, 20]). A includes not only any possible

difference between anti-Stokes and Stokes cross sections arising from resonance effects (due either to plasmon resonances or to resonant Raman scattering for a resonant analyte), but also the standard wavelength dependence of Raman processes $A_{\omega_\nu} = (\omega_L + \omega_\nu)^4/(\omega_L - \omega_\nu)^4$. ρ can be expressed as:

$$\rho = A \left[\frac{\tau\sigma_S I_L}{\hbar\omega_L} + e^{-\hbar\omega_\nu/k_B T} \right]. \quad (5)$$

This simple model shows that the Stokes-Raman signal always remains linearly dependent on I_L . The anti-Stokes signal also shows a linear dependence with power when pumping is negligible. But when pumping dominates over thermal effects, then I_{aS} varies quadratically with power while the aS/S-ratio is linearly dependent on I_L .

The original work by Kneipp et. al.[13] used rhodamine 6G (RH6G) and crystal violet (CV) (two commonly used SERS active dyes) under 830 nm excitation at room temperature (RT). The argument for pumping was primarily based on two observations: (i) the aS/S-ratios were shown to be larger than expected for a Boltzmann factor, and (ii) the *power dependence* of the signal at RT (where the thermal contribution is likely to dominate, or be important) was quadratic. This observation of a non-linear dependence of the anti-Stokes intensities with power (resulting in a linear dependence in the aS/S-ratio) was thought to provide strong evidence for vibrational pumping in SERS. Further measurements on a DNA-base and carbon nanotubes[17] supported these initial results. The arguments against this original interpretation are summarized in the next subsection.

B. Resonance and heating effects

Haslett et. al.[15] were the first to seriously question the existence of vibrational pumping as revealed in the original studies. Extensive measurements were made under similar conditions with a number of both resonant and non-resonant molecules. They observed an anomalous ratio for all the tested resonant molecules which was independent of power until photo-bleaching occurred. No anomaly was observed in the case of the non-resonant molecules. It was concluded that the anomalous ratios observed in the original papers were the result of “hidden” resonances rather than pumping[21]. Brolo et. al.[14] also concluded that the observed anomalous ratio could be explained by resonances. These resonances are accounted for by the asymmetry factor A in the model of the previous section. In the absence of pumping, the aS/S-ratio is predicted to be:

$$\rho = A \exp\left(-\frac{\hbar\omega_\nu}{k_B T}\right). \quad (6)$$

It is clear that the A factor can indeed result in anomalous ratios (different from the Boltzmann factor), even in the absence of pumping.

Furthermore, it was suggested that the observed power dependence was not the effect of pumping but rather laser heating. The effect of heating on ρ in the absence of pumping can be simply understood by including it in Eq. (6). The real temperature of the probed molecule, T_h , may be different to the nominal temperature T because of heating effects, either in the SERS substrate or in the molecule itself [16]. By writing $T_h = T + \Delta T$ and assuming that $\Delta T \ll T$ we can obtain the corresponding ratio, ρ_h , by expanding Eq. 6 as:

$$\rho_h = A \exp\left(\frac{-\hbar\omega_\nu}{k_B T}\right) \exp\left(\frac{\hbar\omega_\nu}{k_B T} \frac{\Delta T}{T}\right). \quad (7)$$

This expression first shows that heating can also result in an anomalous aS/S ratio, even when $A \approx 1$. Moreover, it can have an important impact on the power dependence of ρ , because ΔT should increase with I_L . We can assume in a first approximation that $\Delta T \approx \alpha I_L$, since heat diffusion and transfer are linear problems. The above expression shows that laser heating should then result in an exponential increase of ρ_h with I_L . However, in many cases of interest, the argument in the second exponential is small compared to 1, and Eq. (7) can then be further expanded to give:

$$\rho_h = A \exp\left(\frac{-\hbar\omega_\nu}{k_B T}\right) \left(1 + \frac{\hbar\omega_\nu}{k_B T} \frac{\alpha}{T} I_L\right). \quad (8)$$

A linear dependence of ρ with I_L (or equivalently a quadratic dependence of I_{aS} with I_L) can then equally be the result of conventional heating effects or pumping. Such an observation is therefore insufficient to demonstrate the presence or not of vibrational pumping. We also note that heating effects can also explain the mode-dependent behavior observed in the original work, as the argument of the second exponential in Eq. (7) depends on the mode energy $\hbar\omega_\nu$.

C. Temperature dependence of the aS/S ratios

Most studies have concentrated on finding evidence for SERS pumping at room temperature (RT), in particular by studying the power dependence of the aS/S ratio. It is true that the huge enhancements in SERS conditions greatly increases the contribution from pumping, but may also contribute to an increased heating (in particular directly in the probe molecules). At room temperature (RT) and above, the thermal contribution to ρ is relatively large and in many cases dominates, such that $\rho \approx A \exp(-\hbar\omega_\nu/k_B T)$. The study of vibrational pumping at RT therefore involves measuring small departures from an already existing (large) thermal population. Moreover, as the previous discussion has shown it is also extremely difficult to distinguish the relative contributions or pumping and heating at RT.

A more practical approach is to study the temperature dependence of the aS/S ratios, and in particular the low-temperature regime where thermal effects are expected

to be completely negligible compared to any other mechanisms, and in particular pumping. The temperature dependence can be directly studied using the model presented so far. Figure 1 summarizes the different scenarios for aS/S-ratios as a function of temperature. The solid lines show the variation of the ratio with T when pumping is absent; i.e. an exponential decrease as T decreases, following the Boltzmann factor $\exp(-\hbar\omega_\nu/k_B T)$. The dashed lines show the case when pumping is present. At high T 's the ratio is approximately the same as if pumping were absent. This is the *thermally-dominated regime*. As T is decreased, there is a cross-over to a *pumping-dominated regime*, where the ratio reaches a plateau. We refer to the cross-over temperature between these two regimes as T_{cr} ; indicated by arrows in Fig. 1. The cross-over occurs when pumping and thermal terms in Eq. (5) are comparable, which occurs for:

$$k_B T_{cr} \approx \hbar\omega_\nu \left[\ln \left(\frac{\hbar\omega_L}{\tau\sigma_S I_L} \right) \right]^{-1} \quad (9)$$

The cross-over occurs at a larger temperature for higher powers I_L , for which pumping is stronger, but also for higher energy peaks (with a larger $\hbar\omega_\nu$), for which thermal excitation is weaker.

In the pumping-dominated regime, the aS/S-ratio is constant and equal to $\rho = A\tau\sigma_S I_L/(\hbar\omega_L)$. $I_L/(\hbar\omega_L)$ can be estimated with a good accuracy for a given experimental setup. If $A = 1$ (no asymmetry between σ_S and σ_{aS}) we can therefore deduce the product $\tau\sigma_S$ from the plateau in the aS/S-ratio below T_{cr} . In general, and in particular under SERS conditions, $A \neq 1$, but its value can be determined from the exponential dependence in the thermally-dominated regime (above T_{cr}). In practice, a fit of the experimental data over the whole temperature range with two parameters enables to determine both A and $\tau\sigma_S$, as we shall show later. Nevertheless, the problem of estimating τ still needs to be circumvented to determine the SERS cross-section σ_S itself.

By reducing T , the contribution from pumping becomes dominant, making measurements much easier, and more reliable. It also simplifies greatly their interpretation. But the main advantage is that it enables one to unambiguously rule out heating effects as an alternative explanation. As discussed, the appearance of plateaus for $T < T_{cr}$ in Fig. 1 is a clear characterization of the pumping-dominated regime. Note that it does not mean that there is no heating, but simply that its effect on aS/S-ratios is negligible (because they are dominated by the pumping contribution). Any heating effects may possibly affect the value of T_{cr} , but as long as a plateau is observed, vibrational pumping must occur. Moreover, the value of ρ in the plateau region (from which we will infer SERS cross-sections) is independent of heating.

Studies of the temperature dependence of ρ therefore provide a much clearer evidence for SERS pumping. Notwithstanding, the technique is not without its drawbacks. In order to extract SERS cross-sections for the

method discussed here there are several issues that need special attention. This is the subject of the next section.

III. PRACTICAL ESTIMATION OF CROSS-SECTIONS FROM VIBRATIONAL PUMPING

Several issues need to be considered in the practical determination of SERS cross sections via vibrational pumping. Not all of them can be resolved to a satisfactory degree and *ad-hoc* approximations are needed to obtain estimates of the cross sections. While there is nothing intrinsically wrong with this, it is necessary to be aware of the range of validity of the estimates in order to be able to use them in a different context, or to infer other properties from them. We review these issues in the next subsections.

A. SERS cross-sections

It is worth mentioning here that in most situations in Raman (and in SERS) we talk plainly about the cross section σ while in reality there are at least three possible cross sections we can refer to: (i) radiative, (ii) non-radiative, and (iii) total. In the case of vibrational pumping, for example, the rate at which vibrations are pumped into the molecule is proportional to the *total* cross section. But some of the re-emitted photons might not be observable in the far-field because they are absorbed by plasmon resonances in the vicinity of the probe. This is what makes the distinction between *radiative* and *non-radiative* cross sections. This could lead potentially to inconsistencies among cross sections for different modes if they happen at frequencies where the non-radiative contributions are different. We will not insist in this distinction in what follows, but it is worth keeping in mind that as far as the cross sections is concerned what we measure is the “radiative” part of an effect (pumping) which depends on the “total” (radiative plus non-radiative) cross section. This distinction could be important if inconsistencies are detected.

B. Vibrational lifetimes

We summarize in this subsection the different aspects of the problem of lifetime estimation for the purpose of obtaining SERS cross sections.

- Ultimately, the observation of a cross-over from a thermally-dominated to a pumping-dominated aS/S-ratio leads to an estimation of both the asymmetry factor A and the product $\tau\sigma_S$. An estimation of σ_S itself requires the knowledge of τ , as pointed out before. The latter cannot be directly obtained, in general, from the SERS spectrum. This leads to

a standoff and a serious limitation of this technique. A series of approximations can be justified, to some degree, to obtain an estimation of σ_S regardless of this problem. In the first report of cross section estimation via vibrational pumping[13] a lifetime of $\tau \sim 10$ ps was simply estimated without any reference to the experimental data.

- In order to proceed any further from the obtained value of $\tau\sigma_S$ to an estimation of σ_S itself, we need to make a series of assumptions. The validity of these assumptions needs to be evaluated on a case-by-case basis and the results obtained for the cross section have to be interpreted within these approximations/assumptions.
- Raman peaks in molecules have lineshapes which are seldom pure Lorentzians and have several contributions to their natural widths; a subject of a longstanding history in spectroscopy[22]. The observed linewidth has typically contributions from: (i) groups of Raman modes piled up together in narrow energy regions; (ii) inhomogeneous broadening, (iii) phase coherence relaxation, and (iv) population relaxation. The last two are also known as the *off-diagonal* (dephasing) and *diagonal* (population) relaxation times in density matrix formalism[22], respectively, and are part of the *homogeneous broadening* of the peak. These relaxation times are different from mode to mode and cannot be easily separated from the observed linewidth in a plain SERS spectrum. The *population relaxation* is the one we need (τ) for the estimation of σ_S .
- The presence of multiple modes contributing to a peak is a drawback that can be overcome in many situations. It is not strange in dyes that the observed peaks come from several Raman active modes closely spaced in energy and with different cross sections. This will naturally result in distortions of the lineshape and problems with any estimate of the lifetime based on the width of the peak. This can be overcome by the use of well characterized vibrations which are relatively isolated from the others and even (if possible) complementing the information by density functional theory (DFT) calculations of the Raman spectra[23, 24] to support the selection of those modes that are best candidates for a reliable estimation of τ .
- If the broadening is homogeneous[25], the only remaining contributions to the linewidth are the diagonal and off-diagonal relaxation times. Molecular vibrations have typically very strong anharmonic couplings with other vibrations in the molecule and contributions to inhomogeneous broadenings are mostly negligible. Even in SERS experiments where the single molecule limit is approached[26]

(which would be more sensitive to inhomogeneous broadening) the full width at half maximum (FWHM), Γ , of the peaks does not change by more than $1 - 1.5 \text{ cm}^{-1}$ in peaks with a typical Γ of $\sim 15 - 20 \text{ cm}^{-1}$. The validity of this assumption (whether inhomogeneous broadening is important or not) has to be assessed obviously in each specific situation.

- The separation between diagonal and off-diagonal relaxation times cannot be achieved by a simple SERS spectrum. It is always possible to invoke a different type of spectroscopy (time resolved)[22], but this may not be feasible in most situations. One simple possibility (as done in Ref. [20]) is to estimate the population relaxation by using the FWHM (Γ) of the peaks via $\tau \sim \hbar/\Gamma$; i.e. essentially ignoring the contribution of the dephasing (off-diagonal) relaxation to the width. This will produce an underestimation of τ and an overestimation of σ_S . In addition, this produces typically cross-sections for different peaks which are not entirely consistent with the relative (integrated) intensities among peaks; thus showing an intrinsic inconsistency in the estimation of the τ 's (which can be of the order of a factor of 2 to 10 for the examples we examined). It is generally difficult to make a simple estimation that will be valid for all modes. It is quite clear that for the cross sections to be meaningful (and if they are not affected by different amounts of non-radiative processes) the relative cross sections among peaks must be in accordance with the relative integrated intensities observed in a normal SERS spectrum.
- Population relaxation is caused mainly by the anharmonic coupling to the “thermal bath”. This bath includes all other modes in the molecule as well as those in the solvent or substrate. Generally speaking, higher energy modes have shorter lifetimes due to a greater number of possible decay pathways. Intramolecular anharmonic decays are energy conserving, meaning that high energy modes have more possibilities for a decay than low energy ones. Population relaxation is also the only dynamical process that contributes to the vibrational linewidth in the limit $T \rightarrow 0$.
- It is important to realize that, in principle, *if we find a single peak in the spectrum where the population relaxation can be gained directly from the FWHM via $\tau \sim \hbar/\Gamma$, then all of the cross sections of the other modes follow immediately through the relative integrated intensities of the peaks.* When lacking a time resolved experiment to isolate the contributions properly, *the problem comes down to a judicious choice of a mode where the width is dominated by relaxation population.* A compromise then is to extract the values of the cross sections

by means of the width of the highest (isolated) Raman active mode. A rule of thumb is that the lower the temperature and the higher the energy of the mode the more the linewidth will be dominated by population relaxation. We can then use one mode to estimate its σ_S , and all the others follow automatically from this assumption. The cross sections are now consistent by construction and the method provides, in fact, the means to estimate the relative lifetimes of the modes. We call this procedure the *corrected lifetime method* (CLM).

- If we are comparing different substrates with the same analyte we could also compare directly the values of $\tau\sigma_S$ without any further assumption. If there is no reason to believe that relaxation population is different between the two substrates, *the ratio of $\tau\sigma_S$ for two different substrates provides a direct comparison of SERS cross sections.*

C. The asymmetry factor

- Problems with measuring the asymmetry factor “ A ” can be as important as those to obtain a reliable lifetime. Heating in the thermally-dominated regime can be a *major* problem. As demonstrated in Sec. II B, heating can be in part a source for a larger than normal A , if it is not properly identified.
- Ideally, the best estimation of A can come from measurements at RT with long integration times and very low powers. The obtained A 's should be more or less the same for a given analyte in the presence of the same metal (they are mainly related to the local interaction of the dye with the metal[21]).
- The product $A\tau\sigma_S$ is measured with high accuracy in the pumping dominated “plateau” at low temperatures. Accordingly, the best use of the technique is to use one well-characterized analyte (without photo-bleaching if possible) as a means to compare the relative SERS cross-sections of the dye on different substrates of the same metal, by simple comparison of the plateaus. The product $A\tau\sigma_S$ is perhaps the best “objective” comparison between the cross sections of two substrates without any assumption. However, it is also important to note that the cross sections we are comparing are not the average cross sections but rather a biased average towards the highest cross sections in the sample, as explained in the next subsection.

D. Which cross section do we really measure?

There are additional complications with the estimation of the cross section. It is generally accepted that SERS

signals are dominated by the presence of “hot-spots” or places with high local enhancements. The formulae presented above made implicitly the assumption that the cross section is the same for all N molecules in the sample. The question we want to address now is: do we obtain an estimate of the average cross section with this method? We shall show in what follows that what we actually obtain from the experiment is an estimate which is heavily biased towards the sites with the highest enhancements; i.e. the method provides an estimate of the enhancements in hot-spots. This is of course an advantage and a disadvantage at the same time. We show this explicitly in this section.

We consider a number of molecules (i from 1 to N) in the sample. Each molecule can have a different anti-Stokes, (σ_{aS}^i) and Stokes (σ_S^i) SERS cross sections (according to the asymmetry factor $A^i = \sigma_{aS}^i/\sigma_S^i$ for that molecule). We assume for simplicity that the incident power I_L is the same for all. The rate equation for the average phonon population n^i of a vibrational mode of *one molecule*, i , and its stationary state solution are given by expressions similar to Eqs. (1) and (2): Following the other formulae in the previous sections, the Stokes signal for this molecule is simply $I_S^i = \sigma_S^i I_L$, while the anti-Stokes signal is given by: $I_{aS}^i = n^i \sigma_{aS}^i I_L$. The anti-Stokes/Stokes ratio *for this molecule*, ρ^i , is given by an expression similar to Eq. (5). If all the molecules experienced the same enhancements, then the total Stokes and Anti-stokes intensities would be $I_S = N I_S^i$ and $I_{aS} = N I_{aS}^i$, and the ratio would be $\rho = \rho_i$. However, if the molecules have different cross sections (SERS enhancements), which is a much more realistic assumption, we then have:

$$I_S = \sum_{i=1}^N \sigma_S^i I_L \quad (10)$$

$$= N \langle \sigma_S \rangle I_L, \quad (11)$$

and

$$I_{aS} = \sum_{i=1}^N \sigma_{aS}^i I_L \left(\frac{\tau \sigma_S^i I_L}{\hbar \omega_L} + e^{-\hbar \omega_v / k_B T} \right) \quad (12)$$

$$= N \langle \sigma_{aS} \sigma_S \rangle I_L \frac{\tau I_L}{\hbar \omega_L} + N \langle \sigma_{aS} \rangle I_L e^{-\hbar \omega_v / k_B T}.$$

All the averages here $\langle \dots \rangle$ are the usual statistical ensemble averages. The aS/S-ratio is then:

$$\rho = I_{aS}/I_S = \frac{\langle \sigma_{aS} \rangle}{\langle \sigma_S \rangle} \left[\frac{\langle \sigma_{aS} \sigma_S \rangle}{\langle \sigma_{aS} \rangle} \tau \frac{I_L}{\hbar \omega_L} + e^{-\hbar \omega_v / k_B T} \right]. \quad (13)$$

Comparing this expression with that obtained previously in Eq. (5), what we called A is now replaced by:

$$A^E = \frac{\langle \sigma_{aS} \rangle}{\langle \sigma_S \rangle}. \quad (14)$$

Note that this is not exactly the average of the A^i 's, i.e.

(A). Moreover, what we measure (instead of $\tau \sigma_S$) is now:

$$\tau \sigma_S^E = \tau \frac{\langle \sigma_{aS} \sigma_S \rangle}{\langle \sigma_{aS} \rangle}. \quad (15)$$

To understand the meaning of σ_S^E (E for Ensemble), we need to understand the sources of non-uniformity. The main variation is in the cross-sections, because of the large differences in SERS enhancements at different locations on the SERS substrate. We typically have values which are, say, $10^3 - 10^6$ larger at hot-spots than in other places. However, for a given molecule, the ratio $A^i = \sigma_{aS}^i/\sigma_S^i$ should not vary as much (at least not by more than one order of magnitude). In fact, this ratio can in a first approximation be taken as a constant, which is an intrinsic property of the adsorbed molecule/Ag complex[21]. Assuming that $A^i = A$ is the same for all molecules, we simply get that $A^E = A$, i.e. the A we measure is the correct one. Moreover, using $\sigma_{aS}^i = A \sigma_S^i$, we can express σ_S^E as a function of σ_S^i only as:

$$\sigma_S^E = \frac{\langle \sigma_S^2 \rangle}{\langle \sigma_S \rangle}. \quad (16)$$

If the distribution of σ_S 's were fairly uniform (for example a Gaussian around an average value with a small standard deviation) then σ_S^E would be a good estimate of the average of the distribution (slightly overestimated). But this is far from reality in SERS conditions. A more realistic situation is to have a small number of molecule at a hot-spot (HS), and a large number of molecules at non-HS positions. For the sake of argument, let us demonstrate the effect on this average by considering 10^3 molecules with one molecule at a HS and 999 molecules at places with much lower enhancements. The expression given above would give:

$$\sigma_S^E = \frac{1/1000 (1(\sigma_S^{\text{HS}})^2 + 999(\sigma_S^{\text{NHS}})^2)}{1/1000 (1(\sigma_S^{\text{HS}}) + 999(\sigma_S^{\text{NHS}}))}. \quad (17)$$

If there is a difference of a few orders of magnitude between the cross sections σ_S^{HS} and σ_S^{NHS} , the numerator is then easily dominated by the one molecule at the HS (due to the square). For the numerator, it is not as clear-cut, it all depends on how much stronger the HS is and how many molecules are at non-HS positions. But overall, the denominator is likely to be dominated by σ_S^{HS} , possibly slightly larger if the second contribution is not negligible. This shows that $\sigma_S^E \approx \sigma_S^{\text{HS}}$, perhaps slightly smaller. A more quantitative argument is only possible if we had a more realistic distribution of SERS enhancements for a given substrate, but the qualitative conclusion is that *pumping experiments provide a good lower estimate of the cross-section of the few molecules experiencing the highest enhancements.*

E. Photo-bleaching

The last aspect we want to briefly touch upon in this analysis of cross section estimations via vibrational pumping is photo-bleaching. The exact mechanisms of photo-bleaching under SERS conditions are still poorly understood and would deserve a full study in itself. Photo-bleaching is particularly important in the method we are describing here because it affects the most those molecules that are at HS's (i.e. exposed to the largest enhancements). At high power densities, for example, the population of molecules at HS's will be bleached and this will change the measured cross section. Studying ρ under photo-bleaching conditions could, in principle, tell us something about this distribution. There is robust experimental evidence that photo-bleaching can complicate the analysis, produce experimental artifacts, and -to a large extent- even decide the answer we obtain from a specific experiment. This is added to several experimental complications in aS/S-ratios which include the fact that sometimes (depending on the dispersion of the spectrometer) the anti-Stokes and Stokes sides cannot be measured simultaneously. This implies a delay between the two measurements and therefore a difference in exposure times to the laser. By choosing a certain power level we are, in a way, selecting the population of HS's that we are going to measure. We shall come back to this problem in the discussion of the results. A rule of thumb is that larger laser spots with low power densities (but sufficient to produce detectable pumping), short integration times, and non-resonant (with the dye) laser excitation, are in general preferable for a more reliable estimate of SERS cross sections. All possible measures should be taken (including the type of scanning used) to address and minimize the undesirable effects of photo-bleaching.

IV. EXPERIMENTAL

We turn now to an experimental demonstration of the principles underlined above. SERS measurements have been performed on substrates formed by dried Ag colloids on silicon. The colloids were prepared using the standard Lee and Meisel technique[27]. SERS active samples were prepared by mixing the colloids with a 20 mM KCl solution in equal amounts. The analytes were then added to give a concentration of 10^{-6} M in each case. A small amount of this solution was then dried on to a silicon substrate. The investigated analytes are rhodamine 6G (RH6G), crystal violet (CV), and 3,3'-diethyloxadicarbocyanine (DODC). Figure 2 shows the basic SERS spectra of the used analytes. We shall show the explicit temperature dependencies of the aS/S-ratios for only a few modes (labelled in Fig. 2) while the tables show additional data for other modes. Samples were mounted in a closed-cycle He-cryostat (CTI-Cryogenics) with temperature control in the range 10 – 300 K. Raman measurements were performed using several laser

lines of a Kr⁺ and Ar⁺-ion lasers which were focused to a 20 μ m diameter spot. The signal was collected using a high-numerical aperture photographic zoom lens (Canon, $\times 10$ magnification) onto the entrance slit of a high-dispersion double-additive U1000 Jobin-Yvon spectrometer coupled to a liquid N₂-cooled CCD detector. Peaks were analyzed using standard Voigt functions with subtracted backgrounds. The variation in the aS/S-ratio with T for each mode was then fitted to Eq. 5. For this purpose, it is convenient to modify the expression to:

$$\ln(\rho) = a + \ln \left[b + e^{-\hbar\omega_\nu/k_B T} \right], \quad (18)$$

where $a = \ln(A)$, and $b = \tau\sigma_S I_L / \hbar\omega_L$ which are the (dimensionless) fitted parameters. The τ 's of the peaks (necessary to obtain the cross sections) are estimated in two different ways following the prescriptions in Sec. III A.

As discussed earlier, it is of critical importance that the sample remains stable over the entire length of the experiment. A range of integration times were used depending on the specific sample and measurement to achieve a good signal to noise ratio for different peaks, but power densities were kept to a minimum compatible with the observation of pumping and exposure to the beam was minimized as much as possible in between changes of T . We used $\sim 30 - 50$ mW spread over the 20 μ m diameter spot. As the rate of photo-bleaching may change with T [28] a suitable power density to ensure reasonable stability must be decided at RT, where the effect is greatest. The relatively large spot and low power densities have the triple advantage of (i) reducing photo-bleaching to a negligible level, (ii) reducing any indirect laser heating effects and (iii) improving the averaging over cluster geometries. Still, even under low power density excitation, the choice of laser line can have an important effect on the measurement. An explicit example is shown in Fig. 3 for RH6G under 514 nm excitation. As explained in the caption, this observation is compatible with a bleaching of the HS's with largest cross sections. Laser lines that are strongly resonant with the probe molecule[21] should be avoided so that the photo-stability of the analyte and the accumulated exposure to the laser do not become an issue in the interpretation and analysis of the data. For that reason, we only concentrate hereafter on results obtained with the 647 and 676 nm lines of a Kr⁺-laser. These two lines are close enough to the visible (to profit fully from SERS enhancements) but, by the same token, they do not produce excessive photo-bleaching for the dyes under consideration here.

V. RESULTS AND DISCUSSION

Having all the theoretical tools from the previous sections, we can now easily scan through several experimental results that demonstrate the method in practice. Figure 4 shows the aS/S-ratios ($\ln(\rho)$) vs. T , as measured

using the 676 nm line, for four modes of each of the investigated analytes. The solid lines represent the best fit to the experimental values using Eq. 18. A series of small imperfections can be seen in the data for some modes, but overall the behavior is very well represented by Eq. 18, with RH6G being the best example. The arrows indicate the cross-over points (T_{cr}) between the thermally-dominated and pumping-dominated regimes for all the investigated modes. T_{cr} occurs at higher T 's for higher energy modes, as expected. The fact that pumping is observed for each of the modes indicates that the effect is fairly general and should be observable for a large number of analytes for as long as σ_S is high enough to make pumping observable at moderate power densities[29].

In order to transform these data into estimates of the cross sections we need to address the different methods of estimating τ . Table I shows the experimental results for RH6G taken with the 676 nm line. For the sake of comparison, we display the cross section by using two different estimations of the τ 's. This gives a better idea of how reliable these numbers are and how differences among them should be interpreted. Table I shows both: (i) the extraction of τ directly from the widths via $\tau \sim \hbar/\Gamma$ (this normally renders cross sections which are not fully consistent with the relative integrated intensities of the peaks), and (ii) the extraction of τ from the highest Raman active mode and the subsequent adjustment of the other cross-sections to agree with the relative integrated intensities (as described in Sec. III A). A column with relative intensities across-sections among modes is also provided for completeness. The anti-Stokes cross sections are obtained through the Stokes ones via the fitted value of the asymmetry parameter A from Eq. 18. These results prove the point that the estimation of the lifetime is a crucial step in this method to transform the experimental values into an estimation of the cross sections themselves. The values should be interpreted within this assumption, and their validity should be assessed on a case-by-case basis. The preferred (more consistent) method is of course the one that ensures the relative cross sections to agree with the relative intensities of peaks; i.e. the corrected τ 's method.

Finally, we can discuss the effect of estimating the cross sections for two different excitation wavelengths. The experiment is somewhat restricted in the choice of excitations (to be compatible with photo-stability) but still provides a hint of resonance contributions to the cross sections with some limitations. Table II shows the cross-sections obtained for RH6G, DODC, and CV for 647 and 676 nm excitations for different modes. All the cross sections were obtained by the corrected lifetime method; i.e. estimating the τ of the Raman active mode with the largest Raman shift, and making the other cross-sections consistent with this value through the relative integrated intensities. It is worth noting that in this latter method we only need (in principle) one temperature dependent aS/S-ratio for the highest Raman active mode (judged to be dominated by population relaxation). This together

with the plain SERS spectrum of the dye is enough to estimate all the cross sections of the modes via the relative integrated intensities. The results will be consistent (by construction) but not necessarily accurate (depending on the one mode that has been chosen to estimate the initial cross section). The main conclusions of these experiments can be summarized as follows: (i) RH6G shows larger cross-sections at 647 than at 676 nm. This is consistent with a resonant increase known to exist in RH6G towards the yellow part of the spectrum[21]. (ii) On the contrary, both DODC and CV experience larger cross-sections at 676 nm, consistent with the maximum of the absorption of these dyes being at longer wavelengths with respect to RH6G and, therefore, having a much more red-shifted resonant interaction than RH6G[21]. (iii) Although there is some variations from mode to mode, it is generally true that CV experiences the largest cross-sections in this near-IR region. Table II summarizes therefore a typical example where the performance of different dyes can be tested through appropriate estimates of the cross sections derived from the method presented in this paper.

VI. CONCLUSIONS

We have presented an in-depth discussion of the state-of-the-art of SERS cross section estimation via vibrational pumping and have given several experimental examples of it. Despite the approximations needed and the intrinsic problems of the technique, it is still an excellent tool (and in many cases possibly the only tool) to extract an estimation of the SERS cross-sections in situations where the number of molecules and hot-spots presents in the sample are not known or are difficult to estimate. The *self-normalizing* nature of the method (with respect to the number of molecules involved) is certainly a major advantage. In addition, we feel that these latter experimental and theoretical developments have moved forward to establish vibrational pumping as a real phenomenon in SERS after almost a decade of controversy about its very existence. One outstanding issue that surely deserves further investigation is the effect of photo-bleaching under SERS conditions (in particular in HS). As we showed in Sec. III B, the fact that this technique produces an estimate of the cross sections which is heavily biased towards HS's provides a unique opportunity to explore their characteristics. This is particularly true in the comparison among different substrates (in which the photo-stability of the analyte plays a special role). A forthcoming study on the topic is in preparation and will be published elsewhere.

VII. ACKNOWLEDGEMENTS

PGE and LFC acknowledge support by EPSRC (UK) under grant GR/T06124. RCM acknowledges partial

support from the National Physical Laboratory (UK) and the hospitality of the MacDiarmid Institute at Victoria

University (New Zealand) where the measurements have been performed.

-
- [1] M. Moskovits, *Rev. Mod. Phys.* **57**, 783 (1985).
- [2] N. M. B. Perney, J. J. Baumberg, M. E. Zoorob, M. D. B. Charlton, S. Mahnkopf, and C. M. Netti, *Optics Express* **14**, 847 (2006).
- [3] M. Green and F. M. Liu, *J. Phys. Chem. B* **107**, 13015 (2003).
- [4] V. P. Drachev, M. D. Thoreson, V. Nashine, E. N. Khalullin, D. Ben-Amotz, V. J. Davission, and V. M. Shalaev, *J. Raman Spect.* **36**, 648 (2005).
- [5] J. B. Jackson, S. L. Westcott, L. R. Hirsch, J. L. West, and N. J. Halas, *Appl. Phys. Lett.* **82**, 257 (2003).
- [6] O. Lyandres, N. C. Shah, C. R. Yonzon, J. T. Walsh, M. R. Glucksberg, and R. P. Van Duyne, *Anal. Chem.* **77**, 6134 (2005).
- [7] M. Larsson and J. Lindgren, *J. Raman Spectrosc.* **36**, 394 (2005).
- [8] A. Rasmussen, and V. Deckert, *J. Raman Spectrosc.* **37**, 311 (2006).
- [9] S. Cinta-Pinzaru, N. Peica, B. Kustner, S. Schlucker, M. Schmitt, T. Frosch, J. H. Faber, G. Bringmann, and J. Popp, *J. Raman Spectrosc.* **37**, 326 (2006).
- [10] J. Binoy, I. H. Joe, V. S. Jayakumar, O. F. Nielsen, and J. Aubard, *Laser Phys. Lett.* **2**, 544 (2005).
- [11] A. V. Szeghalmi, L. Leopold, S. Pinzaru, V. Chis, I. Silaghi-Dumitrescu, M. Schmitt, J. Popp, and W. Kiefer, *Biopolymers* **78**, 298 (2005).
- [12] J. M. Sylvia, J. A. Janni, J. D. Klein, and K. M. Spencer, *Anal. Chem.* **72**, 5834, (2000).
- [13] K. Kneipp, Y. Wang, H. Kneipp, I. Itzkan, R. R. Dasari, and M. S. Feld, *Phys. Rev. Lett.* **76**, 2444 (1996).
- [14] A. G. Brolo, A. C. Sanderson, and A. P. Smith, *Phys. Rev. B* **69**, 045424 (2004).
- [15] T. L. Haslett, L. Tay, and M. Moskovits, *J. Chem. Phys.* **113**, 1641 (2000).
- [16] E. C. Le Ru and P. G. Etchegoin, *Faraday Discussions* **132** (in press).
- [17] P. V. Teredesai, A. K. Sood, A. Govindaraj, and C.N.R. Rao, *Appl. Surf. Sci.* **182**, 196 (2001).
- [18] R. C. Maher, L. F. Cohen, E. C. Le Ru, and P. G. Etchegoin, *Faraday Discussions* **132** (in press).
- [19] R. C. Maher, L. F. Cohen, J. C. Gallop, E. C. Le Ru, and P. G. Etchegoin, *J. Phys. Chem. B* **110**, 6797 (2006).
- [20] R. C. Maher, P. G. Etchegoin, E. C. Le Ru, and L. F. Cohen, *J. Phys. Chem. B* (in press).
- [21] R. C. Maher, J. Hou, L. F. Cohen, F. M. Liu, N. Green, R. J. C. Brown, M. J. T. Milton, E. C. Le Ru, J. M. Hadfield, J. E. Harvery, and P. G. Etchegoin, *J. Chem. Phys.* **123**, 084702 (2005).
- [22] A. Laubereau and W. Kaiser, *Rev. Mod. Phys.* **50**, 607 (1978).
- [23] H. Watanabe, N. Hayazawa, Y. Inouye, and S. Kawata, *J. Phys. Chem. B* **109**, 5012 (2005).
- [24] S. Naumov, S. Kapoor, S. Thomas, S. Venkateswaran, and T. Mukherjee, *J. Mol. Structure (Theochem)* **685**, 127 (2204).
- [25] W. Demtröder, *Laser Spectroscopy* (Springer Verlag, Berlin, 2003).
- [26] E. C. Le Ru, M. Meyer, and P. G. Etchegoin, *J. Phys. Chem. B* **110**, 1944 (2006).
- [27] P.C. Lee, D. Meisel, *J. Phys. Chem.* **86**, 3391 (1982).
- [28] N. P. W. Pieczonka and R. F. Aroca, *Chem. Phys. Chem.* **6**, 2473 (2005).
- [29] Measurements on adenine with these lasers showed no signs of optical pumping suggesting that the cross-section is small relative to the analytes used here.

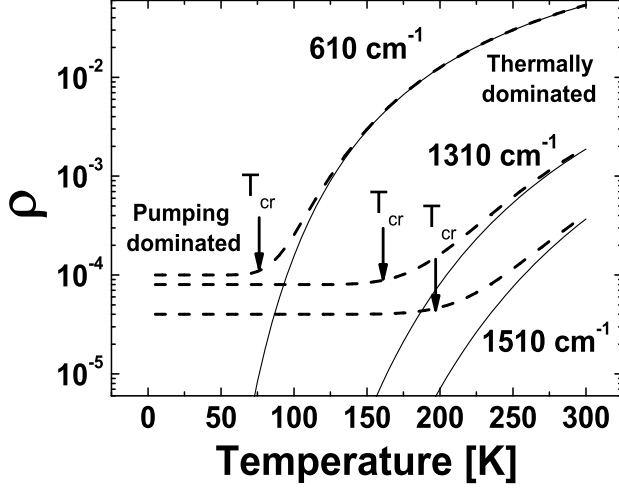


FIG. 1: Schematic diagram showing the temperature dependence of the anti-Stokes/Stokes ratio (ρ) for several different Raman modes. We have assumed here $A = 1$ for simplicity and have used three characteristic Raman modes of RH6G for the example. The solid lines represent the ratio when there is no pumping contribution (Boltzmann factor). The dashed lines show the result of including pumping as given by Eq. 5. There are two regimes, one at high temperature where the thermal contributions dominate and the ratio is similar to what is expected if no pumping were present. The second occurs at low T 's where the contribution of pumping becomes significant relative to the thermal contribution. We refer to the cross-over point between these two regimes as the T_{cr} (indicated by the arrows in this figure). T_{cr} generally occurs at higher T 's for higher energy modes due to the different influence of the exponential factor for different mode energies in Eq. 5. See text for further details.

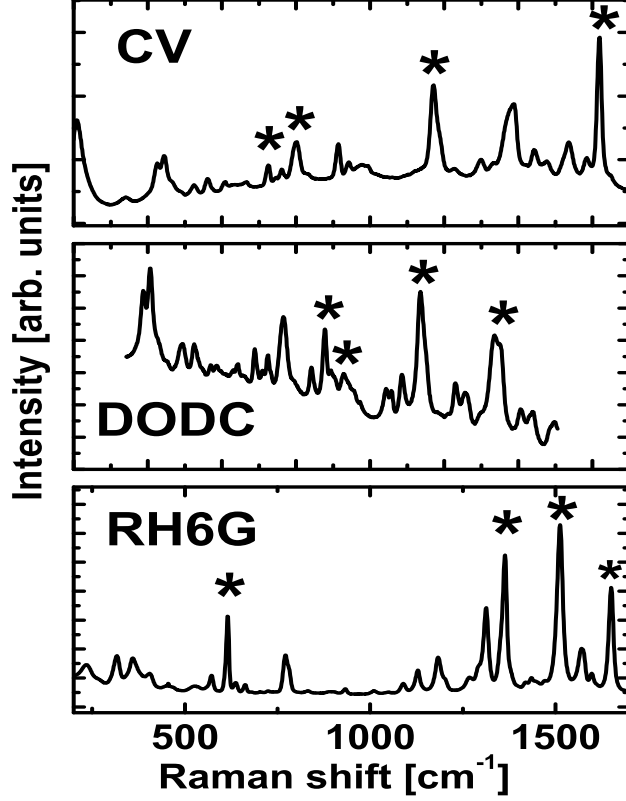


FIG. 2: SERS spectra of the three analytes used in this paper taken with a 633 nm laser: crystal violet (CV, top), 3,3'-diethyloxadicyanine (DODC, center), and rhodamine 6G (RH6G, bottom). The temperature dependence of the aS/S -ratios of the peaks labelled with “*” are explicitly shown in Fig. 4. Table II includes, in addition, estimations of cross sections for additional peaks not labelled here.

Mode (cm^{-1})	b ($\times 10^{-5}$)	τ (ps)	Widths				Corrected				
			Rel. I_S	Rel. σ_S	σ_S (cm^2) ($\times 10^{-15}$)	σ_{aS} (cm^2) ($\times 10^{-15}$)	τ (ps)	Rel. I_S	Rel. σ_S	σ_S (cm^2) ($\times 10^{-15}$)	σ_{aS} (cm^2) ($\times 10^{-15}$)
610	25.6	0.79	1.49	4.86	5.99	22.0	2.6	1.49	1.49	1.84	6.8
780	6.85	0.22	1.82	4.75	5.85	28.2	0.57	1.82	1.82	2.24	11
1360	1.32	0.47	1.72	0.42	0.52	14.3	0.12	1.72	1.72	2.11	58
1510	2.13	0.29	2.98	1.10	0.87	27.2	0.11	2.98	2.98	3.67	114
1650	2.11	0.32	1.00	1.00	1.23	94.8	0.32	1.00	1.00	1.23	95

TABLE I: Values of $b = \tau\sigma_S I_L / \hbar\omega_L$, τ , relative integrated intensities, and cross-sections of the Stokes modes. The values of σ_S and σ_{aS} are shown for two analysis schemes - (i) τ 's obtained from the FWHM of the peaks (ignoring dephasing contributions), and (ii) corrected τ 's to account for the relative integrated intensities. All data are for RH6G using the 676 nm laser line as excitation.

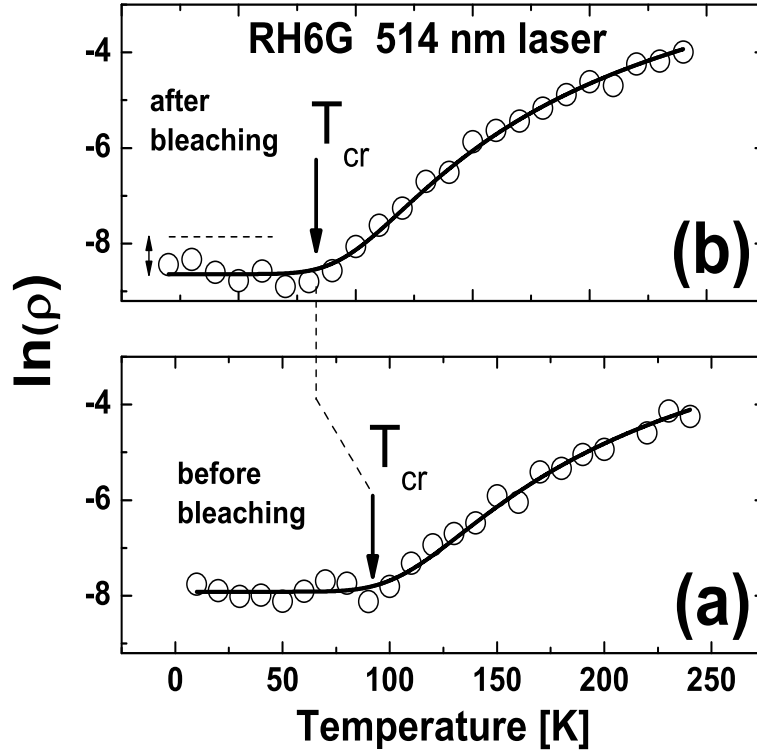


FIG. 3: Effect of photo-bleaching on the temperature dependence of the aS/S-ratio at 514 nm excitation. The measurement in (a) is performed at low power density (25 mW on a $20\ \mu\text{m}$ spot in diameter). The sample is then exposed to 400 mW for 3 min on the same spot and the measurement is repeated afterwards with the same original low power density. The decrease in the plateau of $\ln(\rho)$ to smaller values (and the associated shift of T_{cr} to lower temperatures) in (b) is consistent with a bleaching of the molecules on the HS's with the highest enhancement in the first measurement. The dashed line in (b) is the value at which $\ln(\rho)$ tails in (a). By choosing a certain power level, we are selecting the population of HS's that will survive through the experiment. We are therefore measuring a convoluted property of the substrate and the photo-stability of the probe.

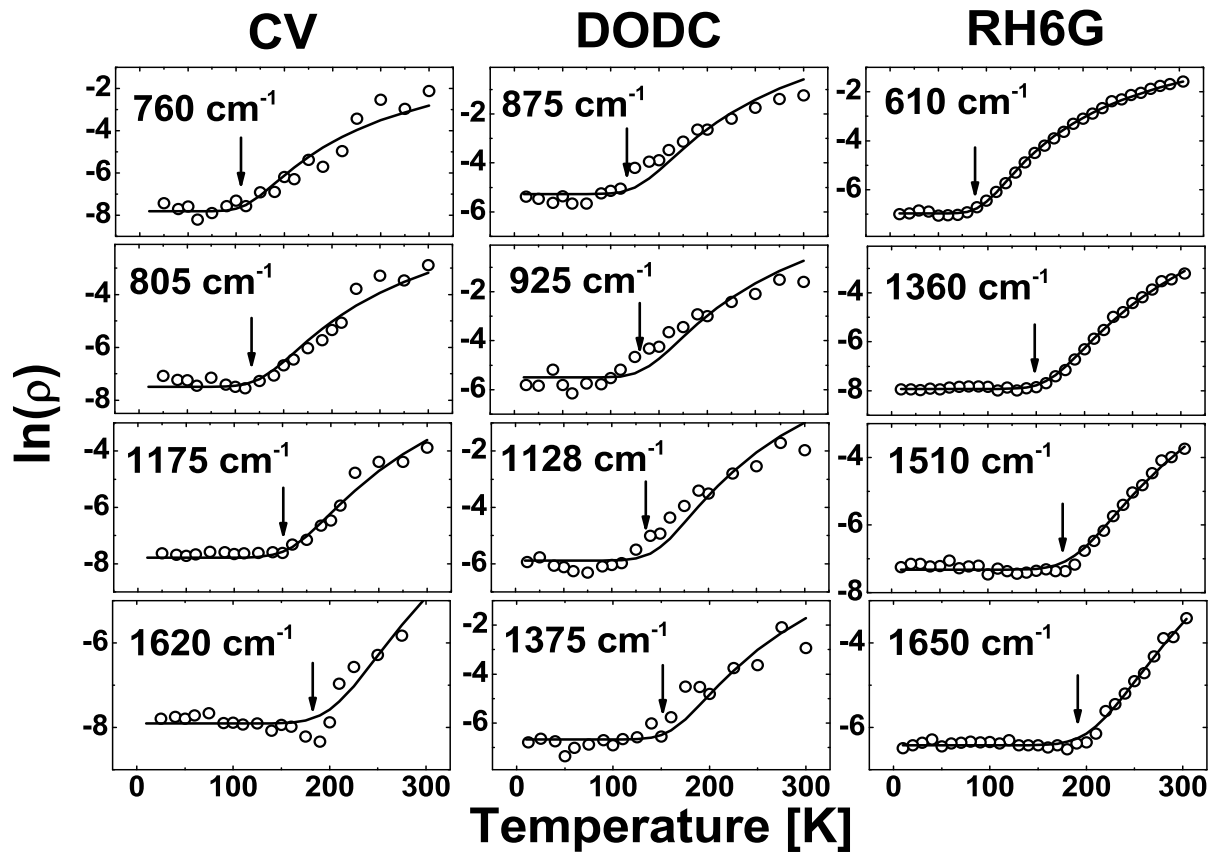


FIG. 4: Anti-Stokes/Stokes ratios ($\ln(\rho)$) as a function of temperature for four modes of each of the analytes investigated here (all taken using 676 nm excitation). The arrows indicate the crossover points between the thermally-dominated and pumping-dominated regimes. Note that the cross over occurs at different temperatures for different modes, being at higher T 's for larger vibrational energies. The solid lines represent the best fit to the experimental data using Eq. 18. Table II presents an analysis of these data using different assumptions for the lifetimes.

Mode (cm^{-1})	647 nm			676 nm		
	σ_S (cm^2) ($\times 10^{-15}$)	σ_{aS} (cm^2) ($\times 10^{-15}$)	b ($\times 10^{-5}$)	σ_S (cm^2) ($\times 10^{-15}$)	σ_{aS} (cm^2) ($\times 10^{-15}$)	b ($\times 10^{-5}$)
RH6G						
610	20.5	112	44.8	1.84	6.75	25.6
780	24.9	136	25.9	2.24	10.8	6.85
1360	2.35	463	1.26	2.11	57.8	1.32
1510	4.08	499	6.38	3.67	114	2.13
1650	13.7	232	22.5	1.23	94.8	2.11
DODC						
875	1.78	26.1	11.1	0.90	32.7	3.04
925	1.66	34.4	8.40	0.94	33.1	3.34
970	1.70	34.2	7.32	1.14	54.9	2.17
1128	2.46	50.6	4.93	1.74	143	8.23
1375	1.31	24.5	1.21	1.01	132	0.30
CV						
760	1.38	1.78	93.5	0.19	0.51	53.6
805	10.9	14.5	74.7	3.41	6.67	28.6
910	3.86	6.53	124	1.10	3.95	6.82
1175	19.5	30.7	18.0	4.29	31.8	5.62
1292	3.72	6.32	8.24	1.62	4.85	3.94
1620	6.35	14.4	9.99	2.01	32.7	2.26

TABLE II: Cross-section values for the Stokes and anti-Stokes Raman modes of CV, RH6G and DODC extracted from $b = \tau\sigma_S I_L / \hbar\omega_L$ obtained through fitting the experimental data to Eq. 18 for both the 647 and 676 nm lasers. Only the lifetime of the mode with the largest Raman shift is estimated from its width and the other cross sections are made consistent with this determination via the relative integrated intensities (CLM- or “corrected τ ’s” method in Sec. III A). See the text for further details.